International Journal of Science and Technology (IJST)
ISSN: 3049-1118, Volume- 3, Issue- 3 (July - September 2026)

Histomorphometric Dynamics of the Uterine Compartments Under *Ricinus Communis Linn*, Clomiphene Citrate, and Exogenous Estrogen Interventions

F Shinku[1], MA Wazhi[2], VE Odey[3], P Nyango[4], MB Muhammed[5], CN Edeh[6], NZ Nden[7], SS Gotom[8], JS Kumbet[9], SA Adamu[10], NJ Chuwang[11], YM Usman[12], MO Omolara[13], RJ Kutshik[14], RT Mcneil[15]

[1,2,3,4,5,6,7,11,12&15]Department of Human Anatomy University of Jos, Jos Nigeria
[8]Senior Chief Technologist, Histology Unit, Department of Human Anatomy, University of Jos
[9]Federal Medical Centre, Keffi, Nassarawa State, Nigeria
[10]Department of Community Medicine, Margaret Lawrence University, Abuja, Nigeria
[13]Department of Human Anatomy, Federal University Wukari, Taraba State
[14]Department of Biochemistry, University of Jos, Jos Nigeria.

ABSTRACT

Synthetic endocrine modulators like Clomiphene Citrate (CC) and exogenous estrogens are vital clinical tools for managing infertility, but they exhibit structural paradoxes, such as severe endometrial thinning or hyperproliferative risks. Ethnopharmacological alternatives, notably Ricinus communis Linnaeus (RC), are widely used in traditional medicine as fertility regulators or primitive contraceptives; however, their tissue-specific micro-anatomical dynamics remain poorly characterized. This study compared the histomorphological, histomorphometric, and immunohistochemical effects of RC seed extract, CC, and exogenous estrogen (conjugated oestrogen) on the uterine and ovarian compartments of adult cyclic Wistar rats (Rattus norvegicus). Twenty-eight (28) cyclic female Wistar rats (150 g – 200 g) in the proestrous phase were divided into seven cohorts (n = 4): Negative Control (Normal Saline); Anti-Estrogen Control (Clomiphene Citrate, 0.00071 mg/kg); Combination Group (CC + RC); Positive Control (Conjugated Estrogen, 8.9 µg/kg); and three Ricinus communis lipid-fraction (RICOM 1013-J) groups were administered subcutaneously at 0.6 g/kg, 1.2 g/kg, and 1.8 g/kg body weight for one day, and vaginal cytology was monitored daily for two cycles. Serum concentrations of Follicle-Stimulating Hormone (FSH), Luteinizing Hormone (LH), and Estradiol (E2) were quantified via Enzyme-Linked Immunosorbent Assay (ELISA). Uterine and ovarian tissues were processed for Hematoxylin and Eosin (H&E) staining and immunohistochemical (IHC) localization of Estrogen Receptor Alpha (ERα) and Estrogen Receptor Beta (ERβ). Histomorphometric parameters of uterine luminal thickness, endometrial thickness, myometrial thickness, and perimetrial thickness were quantified using a photoscope with a graticule. Phytochemical screening of the RC extract revealed lipophilic sterols, terpenoids, saponins, anthraquinones, and flavonoids. Exogenous estrogen and Ricinus communis showed treatment-specific uterine changes; only uterine luminal thickness differed

Published: 07 August 2026
DOI: https://doi.org/10.70558/IJST.2026.v3.i3.241314

significantly, with the RC + CC group showing the highest value. Conversely, CC treatment showed lower mean serum FSH and LH values than normal saline, with histological evidence of a thin luminal epithelium and compact endometrial stroma. Ricinus communis extract showed dose-dependent uterine and ovarian effects, with variable ERα and ERβ staining and follicular distributions. These findings demonstrate that Ricinus communis seed extract acts as a potent tissue-specific endocrine modulator. While it shields the uterine compartments from the hyperproliferative risks associated with exogenous estrogen, its profound anti-folliculogenic and anovulatory actions in the ovary support further investigation of its traditional use as a primitive contraceptive agent.

Keywords: *Ricinus communis*, Clomiphene Citrate, Conjugated Oestrogen, Estrogen Receptor Alpha, Estrogen Receptor Beta, Histomorphometry, Wistar Rats.

Introduction

The mammalian female reproductive system is a highly coordinated biological network governed by the hypothalamic-pituitary-gonadal (HPG) axis (Ayodeji & Roland, 2020). This neuroendocrine cascade regulates the cyclical recruitment, maturation, and release of oocytes, while simultaneously preparing the uterine endometrium for potential embryo implantation (Ayodeji & Roland, 2020). In reproductive toxicology and endocrine research, the adult female Wistar rat (*Rattus norvegicus*) serves as an invaluable classical model due to its short, predictable, and well-characterized estrous cycle (Ayodeji & Roland, 2020). While the human menstrual cycle averages 28 days, the rat estrous cycle lasts typically 4 to 5 days, exhibiting rapid fluctuations in ovarian sex steroid concentrations across four consecutive phases: proestrus, estrus, metestrus, and diestrus (Ayodeji & Roland, 2020; Pu et al., 2024).

Proestrus represents the pre-ovulatory phase characterized by a dramatic surge in luteinizing hormone (LH), follicle-stimulating hormone (FSH), and 17β-estradiol secreted by developing ovarian antral follicles (Mitra et al., 2021). Estrus is the phase of sexual receptivity where ovulation occurs, directly mediated by the peak and subsequent decline of these ovarian hormones (Yoest et al., 2019). Metestrus and diestrus function as the post-ovulatory luteal phases dominated by progesterone secretion from newly formed corpora lutea; if fertilization does not occur, the cycle transitions back into the next follicular wave (Yoest et al., 2019).

Ovarian steroid hormones, particularly estrogens, exert their physiological effects by binding to specific intracellular receptors belonging to the nuclear receptor superfamily of transcription factors (Farzaneh & Zarghi, 2016). There are two distinct classes of estrogen receptor subtypes: Estrogen Receptor Alpha (ERα, encoded by the *Esr1* gene) and Estrogen Receptor Beta (ERβ, encoded by the *Esr2* gene) (Farzaneh & Zarghi, 2016). ERα is the predominant subtype expressed in the uterus, localized within the endometrial stroma, luminal epithelium, and myometrium, where it acts as the primary driver of uterine development and cellular proliferation (Sanchez et al., 2011). In contrast, ERβ is highly abundant in the ovary, located almost exclusively within the granulosa cells of developing follicles, where it plays an indispensable role in normal folliculogenesis and follicle maturation (Farzaneh & Zarghi, 2016; Sanchez et al., 2011). Under normal physiological conditions, ERβ acts as a natural biochemical antagonist or brake to ERα-mediated cellular growth; maintaining a precise homeostatic ERα/ERβ ratio is fundamental to preserving normal reproductive function and

preventing pathological transformations, such as endometrial hyperplasia or carcinogenesis (Farzaneh & Zarghi, 2016).

In modern clinical medicine, systemic administration of synthetic or exogenous estrogenic agents is routinely deployed to manage infertility, ovulatory dysfunction, and menopausal symptoms (Farzaneh & Zarghi, 2016; Nakagawa et al., 2014). However, systemic administration of exogenous estrogen can induce robust, ERα -mediated hyperproliferation in uterine tissues (Mbi Feh et al., 2024). Conversely, Clomiphene Citrate (CC), a non-steroidal triphenylethylene derivative, stands as a first-line clinical treatment for anovulatory infertility, particularly in polycystic ovary syndrome (PCOS) (Mbi Feh et al., 2024). Clomiphene citrate acts as a Selective Estrogen Receptor Modulator (SERM), displaying tissue-specific estrogenic or anti-estrogenic properties (Mbi Feh et al., 2024; Ashrafi et al., 2005). At the level of the hypothalamus, it acts as a competitive antagonist, blocking endogenous estrogen feedback, thereby increasing GnRH pulse frequency and triggering an increased secretion of gonadotropins (LH and FSH) to stimulate ovarian follicular development (Wolf, 2000). However, clomiphene citrate possesses a clinical paradox: despite high ovulation induction rates, the resulting pregnancy rates remain disproportionately low (Nakagawa et al., 2014; Nakamura et al., 1997). This discrepancy is primarily attributed to the lingering anti-estrogenic effects of CC at the level of the uterus, which frequently thins the uterine endometrium and impairs endometrial receptivity, leading to implantation failure (Nakagawa et al., 2014; Nakamura et al., 1997).

Due to the side effects, costs, and accessibility issues associated with conventional endocrine therapies, global attention has shifted toward ethnopharmacology and alternative medicine (Farzaneh & Zarghi, 2016). Phytoestrogens are plant-derived, non-steroidal compounds that possess structural similarities to 17β-estradiol (Farzaneh & Zarghi, 2016). Their molecular mimicry allows them to bind directly to estrogen receptors, acting as either weak agonists or competitive antagonists depending on the specific tissue architecture and receptor subtype present (Kuiper et al., 1998; Patisaul & Jefferson, 2010). *Ricinus communis* Linnaeus, commonly known as the Castor bean plant, is a widespread medicinal plant deeply rooted in traditional African medicine for treating female reproductive conditions (Brahmi et al., 2025). Various parts of the plant, particularly its seed extracts, have been historically documented to possess diverse reproductive bioactivities, functioning interchangeably as fertility regulators or primitive contraceptives (Brahmi et al., 2025).

Phytochemical screening of *Ricinus communis* extracts reveals a complex matrix of bioactive secondary metabolites, including flavonoids, alkaloids, and phytosterols, which are documented to exert potent anti-fertility effects within the female reproductive system when administered at specific doses (Joshua et al., 2020). Despite its widespread traditional use, scientific data regarding how *Ricinus communis* interacts at a molecular level with specific estrogen receptor subtypes (ERα and ERβ) within cyclic reproductive tissues remain heavily fragmented and poorly characterized (Yang et al., 2015; Raji et al., 2006). To truly understand the tissue-specific and cellular impacts of these interventions, macro-level organ analysis is insufficient (Miller et al., 2024).

Immunohistochemistry (IHC) serves as a paramount analytical bridge in modern reproductive morphology by combining histological, immunological, and biochemical techniques to visualize and localize specific antigen-antibody interactions within preserved tissue architectures (Taylor & Rudbeck, 2013). Coupled with histomorphometric analysis, IHC provides an exceptionally sensitive, spatially resolved map of receptor dynamics and compartment modifications (McCarty et al, 1985). This study therefore aims to determine the comparative histomorphometric dynamics and immunohistochemical expressions of ERα and ERβ within the uterine and ovarian compartments of adult cyclic Wistar rats under *Ricinus communis* seed extract, clomiphene citrate, and exogenous estrogen interventions.

MATERIALS AND METHODS

Plant Materials and Extraction

Fresh seeds of *Ricinus communis* Linnaeus were collected from secure botanical sites, authenticated by a certified taxonomist, and deposited in the university herbarium. The seeds were air-dried at room temperature (25°C) and pulverized into a fine powder using an electric blender. The extraction of *Ricinus communis* seeds was carried out according to the sequential solvent fractionation method (Okwuasaba et al.,1991). 100 g of dried seed was pounded and set up for extraction in 150 mL N-Hexane for 75 h at 50°C. The mean yield of 70 ± 2.8 g obtained was mixed with equal volume of diethyl ether and the ether was then removed by warming the extract at 65°C over a warm water bath.

- The crude extract was further partitioned to isolate the specific anticonceptive/bioactive lipid fractions:
- The residue was thoroughly washed and partitioned with n-hexane to separate the ether/hexane-soluble lipid fraction from the insoluble components.

This fraction, conventionally referred to as the RICOM 1013-J fraction was evaporated to a concentrated, clear, viscous oil. The yield of 45 g was dissolved in appropriate volumes of corn oil for subcutaneous (SC) administration.

Phytochemical Screening

Qualitative phytochemical screening of the crude seed extract were performed using standard analytical protocols (Joshua et al., 2020). The extract was screened for the presence of secondary metabolites, including alkaloids (Mayer's and Dragendorff's tests), flavonoids (Shinoda test), tannins (ferric chloride test), saponins (frothing test), and phytosterols (Liebermann-Burchard test).

Experimental Animals and Ethical Approval

Twenty-eight (28) healthy, non-pregnant adult female Wistar albino rats (*Rattus norvegicus*), weighing between 150 g – 200 g, were utilized. The animals were housed in clean polypropylene cages under controlled environmental conditions with a 12-hour light/dark cycle. The rats were provided standard pelletized feed and water *ad libitum*. All experimental procedures were approved by the Institutional Animal Care and Use Committee with Ethical Reference number UJ/FPS/F17-00379 and conducted in strict compliance with international guidelines for the care and use of laboratory animals. Only female rats demonstrating at least

three regular, consecutive 4-day estrous cycles via daily vaginal cytology screening were selected for the baseline experimental cohorts (Marcondes et al., 2002).

Experimental Design and Animal Grouping

Rats in their proestrous phase were randomly divided into 7 groups (n=4 per group) and treatments were administered for 1 day.

1. **Group 1 (Negative Control):** Normal Saline.
2. **Group 2 (Anti-Estrogen Control):** Clomiphene citrate (0.00071 mg/kg body weight).
3. **Group 3 (Combination Treatment):** Clomiphene citrate (0.00071 mg/kg + *Ricinus communis* 1.2 g/kg)
4. **Group 4 (Positive Control):** Exogenous Conjugated Estrogen (8.9 µg/kg body weight).
5. **Group 5 (Test Group 1):** Low-dose *Ricinus communis* extract (0.6 g/kg body weight).
6. **Group 6 (Test Group 2):** Mid-dose *Ricinus communis* extract (1.2 g/kg body weight).
7. **Group 7 (Test Group 3):** High-dose *Ricinus communis* extract (1.8 g/kg body weight).

Hormonal Assay

Twenty-four (24) hours after a two-cycle cyclicity period, all animals were humanely anesthetized. Blood samples were collected via cardiac puncture into non-anticoagulant tubes. The blood was allowed to clot at room temperature for 30 minutes and centrifuged at 1000 rpm for 10 minutes to separate the serum. Serum concentrations of Follicle-Stimulating Hormone (FSH), Luteinizing Hormone (LH), and Estradiol (E2) were quantified using standard enzyme-linked immunosorbent assay (ELISA) test kits according to the manufacturer's instructions.

Tissue Processing and Histology

Following blood collection, the animals were euthanized via cervical dislocation. The reproductive organs (the ovaries and the uterus) were immediately excised, cleared of adherent fat and fixed in 10 % neutral buffered formalin for 48 hours. The tissues were dehydrated through a graded series of ethanols, cleared in xylene, and embedded in paraffin wax. Serial sections were cut at a thickness of 5 µm using a rotary microtome. Representative sections from each group were stained with standard Hematoxylin and Eosin (H&E) for histomorphological and histomorphometric evaluations under a light microscope (Bancroft & Gamble, 2008).

Histomorphometry and Follicular Counting

Uterine histomorphometric examinations focused on three specific localized zones: the luminal epithelium, glandular epithelium, and endometrial stroma (Sanchez et al., 2011). Digital micrographs were captured, and linear measurements (mm) were obtained using photoscope with calibrated graticule. For each uterine section, uterine lumen, endometrium, myometrium and perimetrium thickness were measured. Ovarian structural evaluation included differential follicular counting (McGee & Hsueh, 2000). Matured and developing follicles were counted based on well-defined morphological criteria using digital software (ImageJ).

Immunohistochemistry for ERs (α and β)

Paraffin-embedded sections (4 µm thick) were deparaffinized and rehydrated. Antigen retrieval was performed by heating sections in 0.01 M citrate buffer (pH 6.0) in a microwave for 15 minutes. Endogenous peroxidase activity was blocked by incubating the slides in 3 % hydrogen peroxide in methanol for 10 minutes. After washing with phosphate-buffered saline (PBS), non-specific binding sites were blocked using 5 % normal goat serum for 30 minutes.

The sections were then incubated overnight at 4°C with specific primary antibodies: rabbit polyclonal anti-ERα (1:100 dilution) and rabbit polyclonal anti-ERβ (1:100 dilution) (Pelletier et al., 2000). After washing with PBS, sections were incubated with biotinylated secondary antibodies for 30 minutes, followed by streptavidin-horseradish peroxidase (HRP) complex for 30 minutes. Immunoreactivity was visualised using 3,3′-Diaminobenzidine (DAB) substrate solution, and sections were counterstained with Mayer's hematoxylin.

Qualitative Scoring Systems

Under brightfield microscopy, standard tissue fields are classified based on the visual attributes of the brown DAB precipitate (Varghese et al., 2014; Fedchenko & Reifenrath, 2014):

1. Negative (**-** or Score 0): Complete absence of brown DAB precipitate within the specific cell population. The tissue matrix displays only the blue/purple hematoxylin counterstain, matching the negative control slides.
2. Weak / Low Positive (+ or **1**+): Faint, light-yellowish to tan staining that is poorly visible at low power but distinguishable at high magnification (400×). The signal is often confined to isolated patches or individual cellular borders.
3. Moderate Positive (++ or **2**+): Clear, distinct golden-brown staining easily identifiable at intermediate magnification (100× to 200×) that tracks reliably across continuous bands of target cells.
4. Strong/High Positive (+++ or **3**+): Deep, intense dark-brown to blackish-brown heavy precipitate that is readily visible at low magnification (40×). The precipitate completely occupies the target cellular compartment (nuclear, cytoplasmic, or membranous) and may obscure background nuclear detail.

Statistical Analysis

Quantitative data, including hormonal concentrations and histomorphometric dimensions are expressed as Mean ± Standard Deviation (SD). Statistical analyses were performed using statistical software. Differences between experimental groups were analyzed using One-way Analysis of Variance (ANOVA). Ovarian follicle distribution frequencies were compared using the Chi-square test. Values of $p < 0.05$ were considered statistically significant.

RESULTS

Phytochemical Constituents of *Ricinus communis* Seed Extract

Phytochemical screening of the n-hexane seed extract confirmed the presence of lipophilic sterols (steroids), terpenoids, saponins, anthraquinones, and flavonoids. Crucially, the n-hexane

screening excluded hydrophilic alkaloids and phenols, confirming that the extract represents a purely non-polar lipid fraction (RICOM 1013-J) of the seed.

Serum Hormonal Profiles

Table 1: Hormonal Profiles of Luteinizing Hormone (LH), Follicle Stimulating Hormone (FSH) and Estradiol (E2)

Experimental Groups	Normal Saline	Clomid	RC + Clomid	Conj. Oestrogen	RC (0.6 g/kg)	RC (1.2 g/kg)	RC (1.8 g/kg)
LH (mIU/ml)	20.13 ± 1.89	13.35 ± 0.93^{a}	7.00 ± 0.81^{ab}	29.58 ± 2.23^{abc}	31.40 ± 2.84^{abc}	24.20 ± 4.57^{bc}	7.45 ± 0.74^{abdef}
FSH (mIU/ml)	17.30 ± 1.64	11.50 ± 0.80^{a}	6.00 ± 0.74^{ab}	25.40 ± 1.93^{abc}	27.50 ± 2.33^{abc}	20.80 ± 3.96^{bc}	6.43 ± 0.66^{abdef}
E2 (pg/ml)	51.07 ± 4.67	76.83 ± 5.40	150.70 ± 19.24^{ab}	34.73 ± 2.46^{bc}	32.10 ± 2.71^{bc}	43.65 ± 10.07^{b}	138.30 ± 14.47^{abdef}

Values are expressed as Mean ± SD (standard deviation). LH = Luteinizing Hormone (mIU/ml), FSH = Follicle Stimulating Hormone (mIU/ml), and Estradiol = E2 (pg/ml). Superscripts indicate statistically significant differences at $p < 0.05$, where ^{a} denotes comparison with Normal Saline, ^{b} with Clomid, ^{c} with RC + Clomid, ^{d} with Conjugated Oestrogen, ^{e} with RC (0.6 g/kg), ^{f} with RC (1.2 g/kg), and ^{g} with RC (1.8 g/kg).

Table 1 displays the effects of RC (at dosages of 0.6, 1.2, and 1.8 g/kg), Clomid, RC combined with Clomid, and conjugated oestrogen on the hormonal profiles of experimental groups compared to a normal saline control. The parameters measured include Luteinizing Hormone (LH), Follicle Stimulating Hormone (FSH), and Estradiol (E2), with results expressed as Mean ± SD. Analysis shows that RC at 0.6 g/kg (LH: 31.40 ± 2.84; FSH: 27.50 ± 2.33) and conjugated oestrogen (LH: 29.58 ± 2.23; FSH: 25.40 ± 1.93) were significantly higher ($p < 0.05$) than Normal Saline and Clomid, but not significantly different from each other; RC (1.2 g/kg) (LH: 24.20 ± 4.57; FSH: 20.80 ± 3.96) did not differ significantly from Normal Saline or conjugated oestrogen but was significantly higher than Clomid and RC + Clomid; Clomid (LH: 13.35 ± 0.93; FSH: 11.50 ± 0.80) was significantly lower than Normal Saline, conjugated oestrogen, and RC (0.6 and 1.2g/kg) but higher than RC + Clomid; RC + Clomid (LH: 7.00 ± 0.81; FSH: 6.00 ± 0.74) and RC (1.8g/kg) (LH: 7.45 ± 0.74; FSH: 6.43 ± 0.66) were not significantly different from each other but were significantly lower than all other groups. For Estradiol (E2), RC + Clomid (150.70 ± 19.24 pg/ml) and RC (1.8g/kg) (138.30 ± 14.47 pg/ml) were not significantly different from each other but were significantly higher ($p < 0.05$) than Normal Saline (51.07 ± 4.67 pg/ml), Clomid (76.83 ± 5.40 pg/ml), conjugated oestrogen (34.73 ± 2.46 pg/ml), RC (0.6g/kg) (32.10 ± 2.71 pg/ml), and RC (1.2g/kg) (43.65 ± 10.07 pg/ml); Clomid did not differ significantly from Normal Saline but was significantly higher than conjugated oestrogen, RC (0.6g/kg), and RC (1.2g/kg), while no significant differences were observed among Normal Saline, conjugated oestrogen, RC (0.6g/kg), and RC (1.2g/kg).

Histomorphometric Alterations in Uterine Compartments

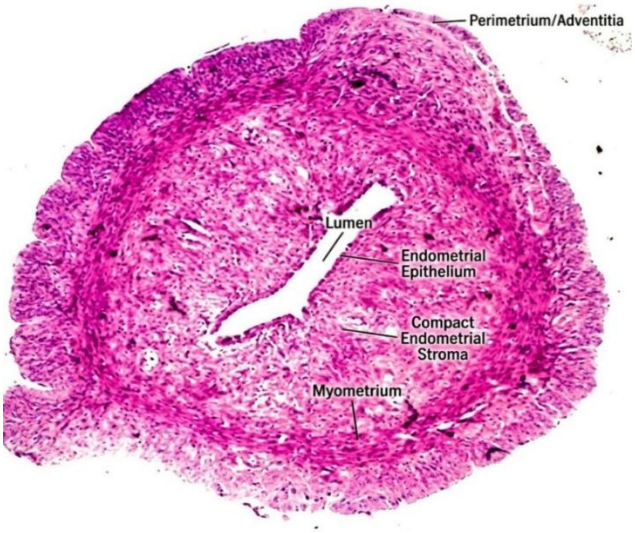

Plate 1 Photomicrograph of uterus treated with normal saline (Control) showing Endometrial Lumen (EL), Endometrial Epithelium (EE), Compact Endometrial Stroma (CES), Myometrium (M) and Perimetrium (P). (H & E x 40)

The photomicrograph of the uterus treated with normal saline (control) reveals a normal histological architecture. The endometrial lumen (EL) is lined by a distinct endometrial epithelium (EE) showing well-organized structures, while the myometrium (M) displays tightly packed smooth muscle fibers and the perimetrium (P) forms the outermost serosal layer. No pathological changes, such as hemorrhage or degeneration, are evident, indicating a healthy uterine structure. This baseline morphology serves as a reference for comparing treatment-induced alterations in other groups, confirming the absence of external influences in the control.

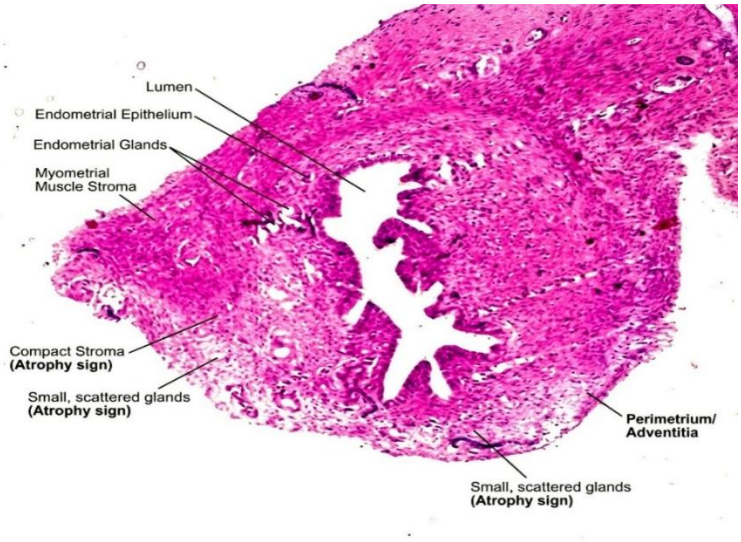

Plate 2 Photomicrograph of uterus treated with 0.00071 mg/kg body weight of clomiphene citrate showing Endometrial Lumen (EL), Endometrial Epithelium (EE), Endometrial Glands (EG), Myometrium (M), and Perimetrium (P). (H & E x 40)

The uterus treated with 0.00071 mg/kg Clomiphene Citrate shows the endometrial lumen (EL), endometrial epithelium (EE), and endometrium (E) with few and scattered endometrial glands (EG) embedded in the stroma and the stroma appearing more compact. This is consistent with a quiescent, atrophic endometrial lining under Clomid-like suppression.

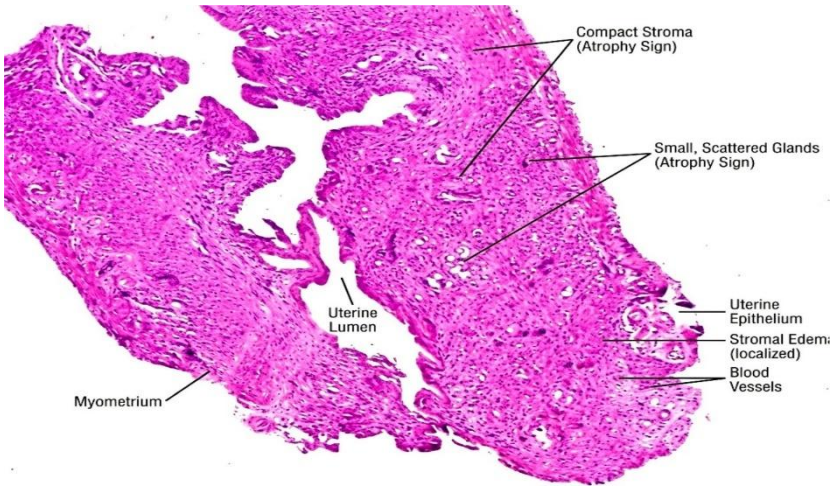

Plate 3 Photomicrograph of uterus treated with 0.00071 mg/kg body weight of Clomiphene Citrate and 1.2 g/kg body weight of *Ricinus communis* showing Endometrial Lumen (EL), Endometrial Epithelium (EE), Compact Endometrial Stroma (CES), Myometrium (M), Endometrial Glands (EG), Blood Vessels (BV) and Perimetrium (P). (H & E x 40)

This specimen exhibits endometrial atrophy, characterized by a severely compact stroma, very small and scattered endometrial glands (indicating low activity), and a simplified, thin epithelium. The changes are more pronounced than with Clomid alone, showing an enhanced suppressive effect from the combined treatment.

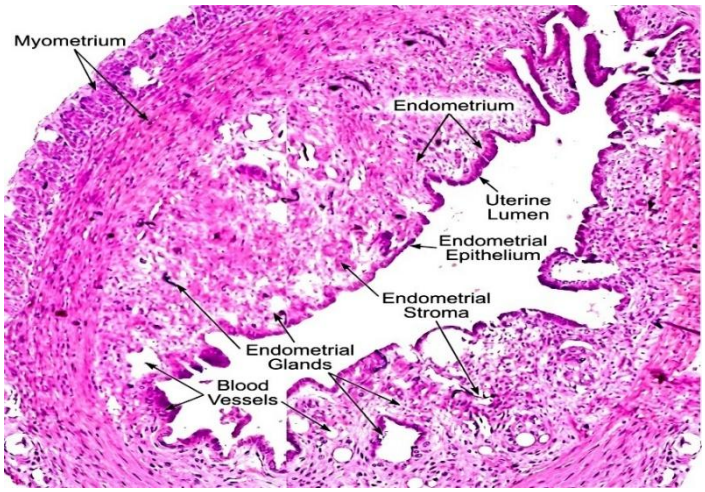

Plate 4 Photomicrograph of uterus treated with 8.9 µg/kg body weight of conjugated estradiol showing Uterine Lumen (UL), Endometrial Epithelium (EE), Endometrium (E), Myometrium (M), Endometrial Glands (EG) and Blood Vessels (BV). (H & E x 40)

The uterus exhibits advanced endometrial atrophy, characterized by a thin and inactive epithelial lining, a highly compact and dense stroma, and a reduction in the size, complexity and number of endometrial glands compared to the normal saline group.

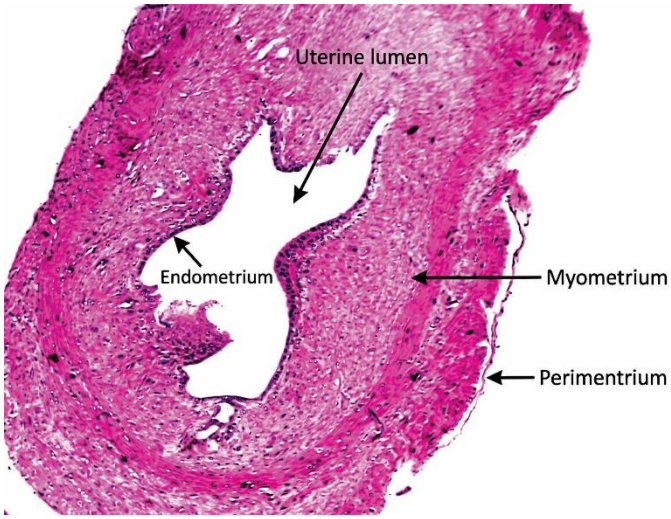

Plate 5 Photomicrograph of uterus treated with 0.6 g/kg body weight of *Ricinus communis* showing Uterine Lumen (UL), Endometrium (E), Myometrium (M) and Perimetrium (P). (H & E x 40)

The tissue above exhibits a relatively narrow, star-shaped lumen lined by a pseudostratified columnar epithelium and thick muscularis externa, comprising three poorly defined, yet distinct layers: an inner longitudinal, a broad middle circular and an outer longitudinal layer. There are no pathological changes noted in this section.

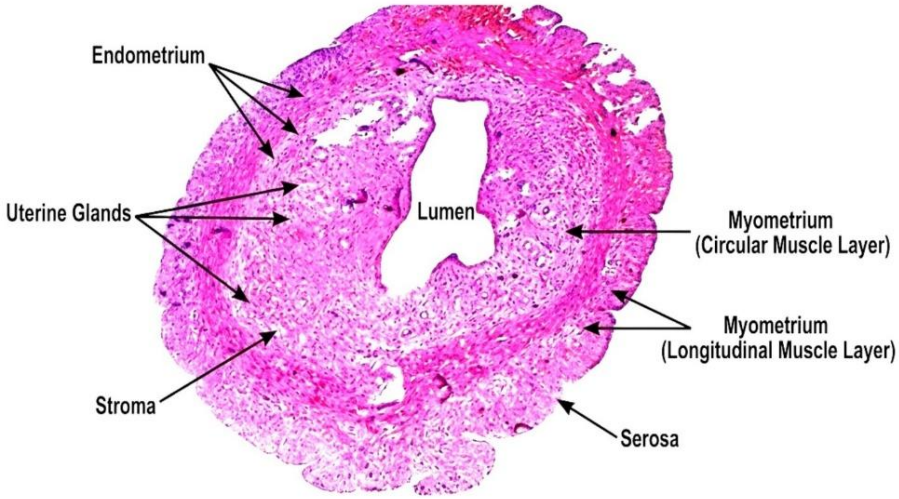

Plate 6 Photomicrograph of uterus treated with 1.2 g/kg body weight of *Ricinus communis* showing Uterine Lumen (UL), Endometrium (E), Myometrium (M), Uterine Glands (UG) and Serosa (S). (H & E x 40)

The tissue maintains a largely normal architecture. Normal uterine layers (Endometrium, myometrium and perimetrium) are preserved. The endometrium contains prominent and well-defined uterine glands. The lumen is clear with minimal or no significant pathological changes.

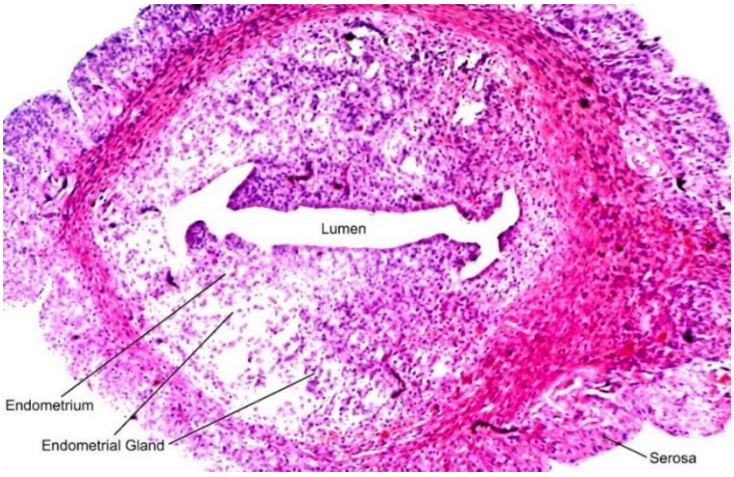

Plate 7 Photomicrograph of uterus treated with *Ricinus communis* 1.8 g/kg body weight showing Uterine Lumen (UL), Endometrium (E), Endometrial Glands (EG) and Serosa (S). (H & E x 40)

The tissue above shows maintained concentric uterine architecture (Lumen, Endometrium, Myometrium layers). The lumen maintains a distinct and complex but irregular. The endometrium shows relatively compact stroma with low to moderate similarity. The prominent uterine glands are notably scarce compared to the control, suggestive of glandular hypoplasia. The myometrium is prominent, thick, well-organized muscular layer. No pathological feature of massive degeneration, atrophy or inflammation.

Table 2: One-way ANOVA of Uterine Lumen (UL), Endometrial Thickness (ET), Myometrial Thickness (MT) and Perimentrial Thickness (PT) measurements

Experimental Groups	Normal Saline	Clomid	RC + Clomid	Conj. Oestrogen	RC (0.6 g/kg)	RC (1.2 g/kg)	RC (1.8 g/kg)
ULL							
Mean ± SD	2.77 ± 1.88	2.55 ± 0.37	3.78 ± 0.25	3.50 ± 0.54	3.43 ± 0.43	3.48 ± 0.40	3.48 ± 0.85
ULT							
Mean ± SD	0.50 ± 0.36	0.95 ± 0.10	2.73 ± 0.21^{abdefg}	0.58 ± 0.05	0.80 ± 0.64	1.15 ± 0.88	0.98 ± 0.17
E							
Mean ± SD	1.60 ± 0.35	2.55 ± 0.17	2.08 ± 0.25	2.33 ± 0.82	1.75 ± 1.15	1.95 ± 0.67	1.95 ± 0.89
M							
Mean ± SD	0.60 ± 0.17	0.65 ± 0.24	0.95 ± 0.17	0.45 ± 0.10	0.60 ± 0.24	0.85 ± 0.97	0.98 ± 0.76
P							
Mean ± SD	0.90 ± 0.17	0.90 ± 0.17	0.90 ± 0.00	0.65 ± 0.10	0.83 ± 0.39	0.85 ± 0.19	0.83 ± 0.15

Superscripts indicate statistically significant differences at $p < 0.05$, where ^{a} denotes comparison with Normal Saline, ^{b} with Clomid, ^{d} with Conjugated Oestrogen, ^{e} with RC (0.6 g/kg), ^{f} with RC (1.2 g/kg), and ^{g} with RC (1.8 g/kg). SD is Standard Deviation.

To evaluate the impact of the experimental treatments on histomorphometric parameters as shown above**,** a one-way ANOVA revealed that statistically significant differences ($p < 0.05$) were observed only in the ULT parameter. The RC + Clomid group (2.73 ± 0.21) showed statistically significant differences when compared with the Normal Saline group (0.50 ± 0.36), Clomid group (0.95 ± 0.10), Conjugated Oestrogen group (0.58 ± 0.05), RC (0.6 g/kg) group (0.80 ± 0.64), RC (1.2 g/kg) group (1.15 ± 0.88), and RC (1.8 g/kg) group (0.98 ± 0.17), as indicated by the superscript annotations. No statistically significant differences were observed for ULL, E, M, or P parameters across the experimental groups. All values are expressed as mean ± standard deviation, with superscripts indicating significant pairwise comparisons.

Ovarian Histomorphology and Follicular Distribution

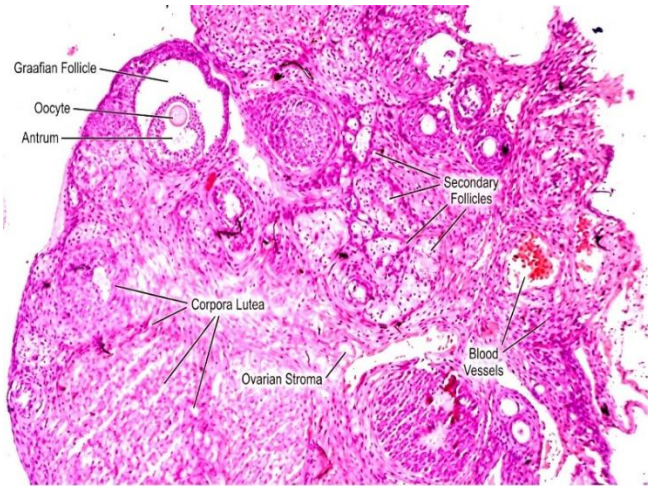

Plate 8 Photomicrograph of Ovary treated with normal saline (Control) showing Secondary Follicles (SF), Blood Vessels (BV), Graafian Follicles (GF), Ovarian Stroma (OS), Corpora Lutea (CL), Oocytes (O) and Antrum (A). (H & E x 40)

The section of Ovary shows normal, multi-stage follicular development. The tissue also shows rich supply of developing follicles and multiple corpora lutea. No morphological changes were observed.

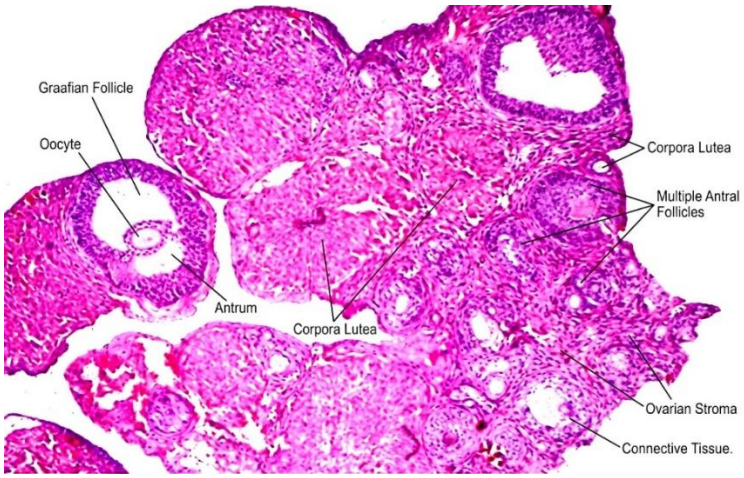

Plate 9 Photomicrograph of Ovary treated with Clomiphene Citrate 0.00071 mg/kg body weight showing Graafian Follicles (GF), Antral Follicles (AF), and Corpora Lutea (CL). (H & E x 40).

The examined section shows large, well-developed corpora lutea (CL) and a high number of developing follicles. The stroma is well-vascularized as compared to normal with a clear increase in the number and development of both follicles and corpora lutea, suggestive of folliculogenesis and ovulation.

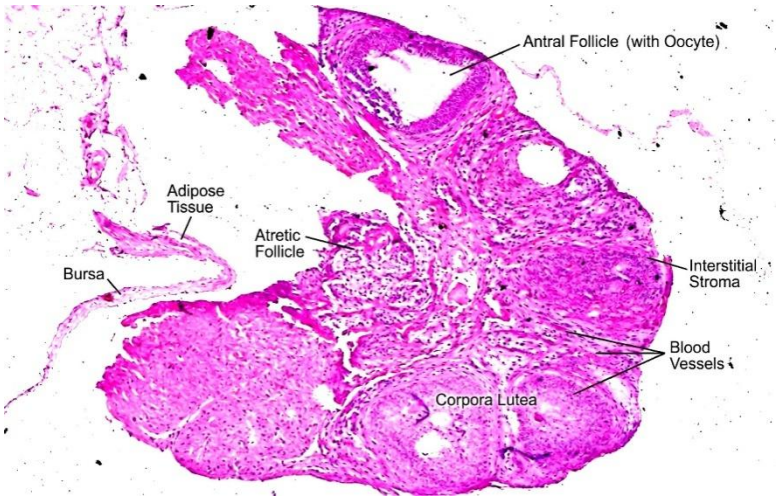

Plate 10 Photomicrograph of Ovary treated with Clomiphene Citrate 0.00071 mg/kg body weight and *Ricinus communis* 1.2 g/kg body weight showing Secondary Follicles (SF), Blood Vessels (BV), Atretic Follicle (AF) and Corpora Lutea (CL) (H & E x 40)

The ovary shows increased vascularization and a higher density of developing ovarian follicles (folliculogenesis). Multiple tertiary and early antral follicles are visible, suggesting stimulated follicular development.

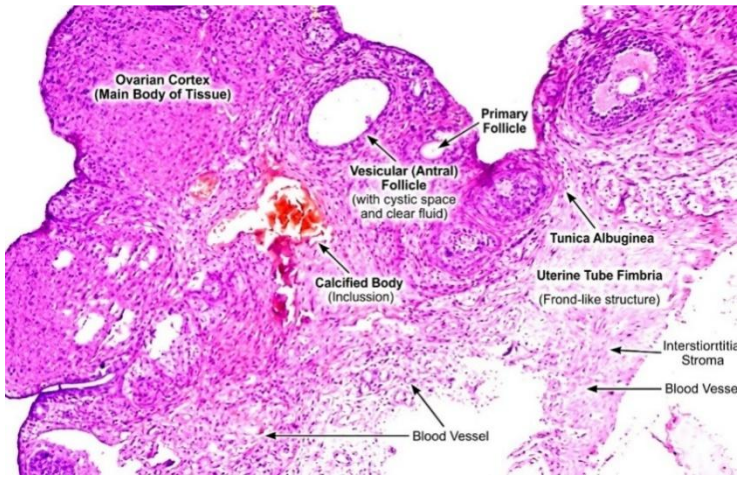

Plate 11 Photomicrograph of Ovary treated with Conjugated oestrogen 8.9 µg/kg body weight showing Primary Follicles (PF), Antral Follicles (AF) and Blood Vessels (BV) (H & E x 40)

The histological image of the ovarian tissue above shows a primary follicle characterized by a single layer of cuboidal granulosa cells surrounding an oocyte. The visible morphological change is the condensation of the oocyte nucleus (pyknosis) and some disorganization of the granulosa cells, which are indicative of early atretic (degenerative) changes. A distinct, dense, calcified body (psammoma body) with some lamellation is visible. The morphology suggests the dystrophic calcification of a previous structure, possibly a degenerated follicle or inclusion.

The vesicular follicle shows an expansive antral (cystic) space with sparse granulosa cells and a lack of a cumulus oophoricus mass, a morphology often associated with non-ovulatory or quiescent follicles.

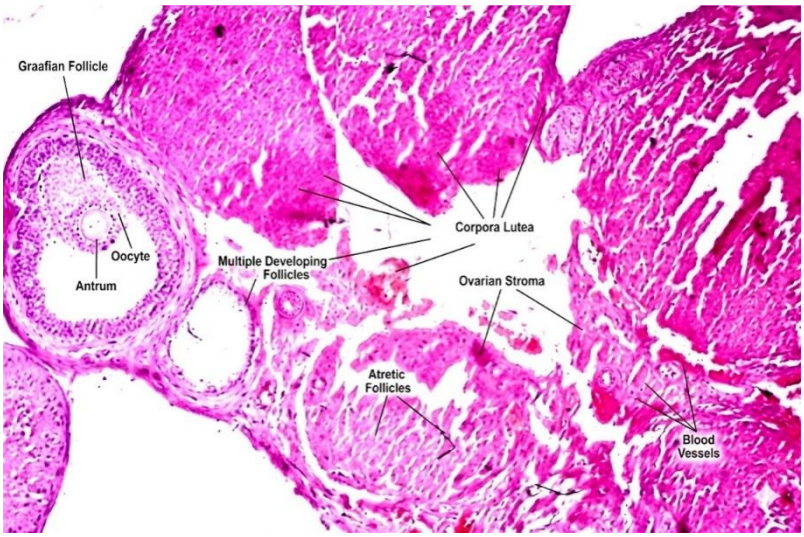

Plate 12 Photomicrograph of Ovary treated with *Ricinus communis* 0.6 g/kg body weight showing Graafian Follicles (GF), Multiple Developing Follicles (MDF), Atretic Follicles (AF), Blood Vessels (BV) and Oocyte (O). (H & E x 40)

The ovary shows a marked increase in atretic follicles. Granulosa cells appear thinner in developing follicles. Stroma and large corpora lutea show signs of altered cellular organization. The Graafian follicle is clear but exhibits some signs of early atresia. These changes suggest potential inhibition of folliculogenesis.

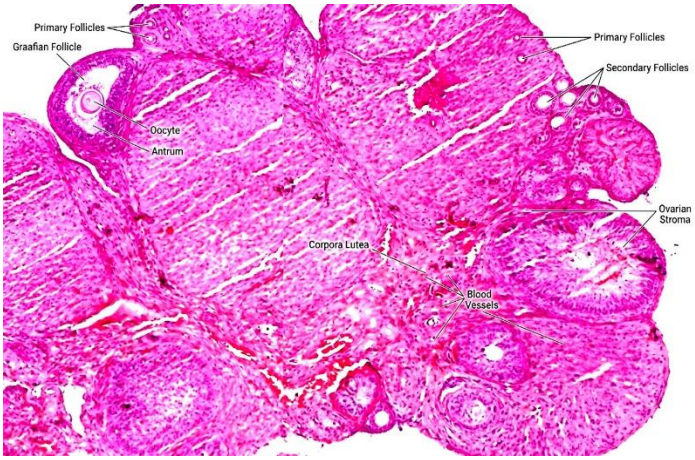

Plate 13 Photomicrograph of Ovary treated with *Ricinus communis* 1.2 g/kg body weight showing Primary Follicles (PF), Blood Vessels (BV), Secondary Follicles (SF), and Oocyte (O). (H & E x 40)

The histological section above shows a healthy ovarian architecture with a complete array of follicular development stages. The prominent Graafian Follicle in the upper left showing a defined oocyte and antrum. The corpora lutea (CL) occupy a significant volume. The stromal matrix is well defined and vascularized.

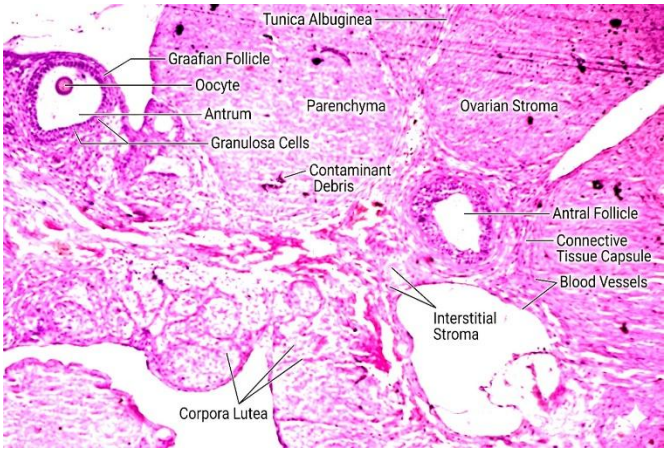

Plate 14 Photomicrograph of Ovary treated with *Ricinus communis* 1.8 g/kg body weight showing Antral Follicles (AF), Blood Vessels (BV), Corpora Lutea (CL), Graafian Follicle (GF), Antrum (A) and Oocyte (O). (H & E x 40)

This histological section shows increase in stromal cell density and noticeable changes in follicular morphology. Several follicles exhibit irregular shapes and loss of distinct cellular layering, indicative of increased atresia. There are some areas of poorly defined follicular boundaries and a disorganized appearance suggestive of treatment-induced changes.

Chi-square showing the follicular distribution among various groups treated with Ricinus communis, Estrogen and Clomiphene Citrate

To evaluate the association between treatment groups and follicular outcomes, a chi-square test of independence was conducted, which revealed a statistically significant relationship as presented in Table 3 ($\chi^2 = 14.92$, df = 6, p = 0.02, Cramer's V = 0.17). The distribution of follicular stages differed across treatments, with the proportion of matured follicles ranging from 31.8% in the Clomid group to 55.6% in the RC (1.8 g/kg b.w.) group, while developing follicles remained predominant in most groups. A progressive increase in matured follicle proportions was observed across the RC dose levels, particularly at higher doses, compared with the normal saline, Clomid, and RC + Clomid groups. The Cramer's V value of 0.171 indicates a small effect size, suggesting a weak but meaningful association between treatment type and follicular outcome. Overall, 41.2% of follicles were matured and 58.8% were developing across all treatment conditions.

Table 3: Distribution of Matured and Developing Follicles Across Experimental Groups

Treatment group	Normal saline	Clomid	RC + Clomid	Conjugated Estrogen	RC (0.6 g/kg b.w.)	RC (1.2 g/kg b.w.)	RC (1.8 g/kg b.w.)	Total
Matured Follicles, n (%)	28 (33.3)	27 (31.8)	15 (36.6)	20 (41.7)	29 (38.2)	47 (48.5)	45 (55.6)	211 (41.2)
Developing Follicles, n (%)	56 (66.7)	58 (68.2)	26 (63.4)	28 (58.3)	47 (61.8)	50 (51.5)	36 (44.4)	301 (58.8)

Total n (%)	84 (100)	85 (100)	41 (100)	48 (100)	76 (100)	97 (100)	81 (100)	512 (100.0)
χ^2	14.92	14.92	14.92	14.92	14.92	14.92	14.92	14.92
df	6	6	6	6	6	6	6	6
P-value	0.02	0.02	0.02	0.02	0.02	0.02	0.02	0.02
Cramer's V	0.17	0.17	0.17	0.17	0.17	0.17	0.17	0.17

Data are presented as number (percentage). χ^2 = chi-square statistic; df = degrees of freedom; Cramer's V = effect size indicating a small association between treatment group and follicular outcome.

Immunohistochemical expression of ERα and ERβ in the uterus and ovary

Table 4: Immunohistochemical DAB Staining Intensities in Uterine Tissue for ERα and ERβ Expression

Treatment Group	Dosing Context	DAB Intensity Score ERα and ERβ	Visual Representation	Molecular Phenotype
Normal Saline (Control)	Baseline vehicle	2 (++)	Moderate Brown	Normal physiological expression
Clomiphene Citrate (CC)	0.00071 mg/kg b.w.	2 (++)	Moderate Brown	Maintained baseline receptor density
CC + *Ricinus communis*	0.00071 mg/kg + 1.2 g/kg	2 (++)	Moderate Brown	Retained expression profile
Conjugated Estrogen	8.9 µg/kg b.w.	2 (++)	Moderate Brown	Sustained structural receptor pool
Ricinus communis	0.6 g/kg b.w.	2 (++)	Moderate Brown	Unaltered peripheral expression
Ricinus communis	1.2 g/kg b.w.	1 (+)	Light / Sparse Brown	Lower staining intensity
Ricinus communis	1.8 g/kg b.w.	2 (++)	Moderate Brown	Moderate staining

Table 5: Ovarian Immunohistochemical DAB Staining Intensities for ERα and ERβ Expression

Treatment Group	Dosing Context	DAB Intensity Score ERα and ERβ	Visual Representation	Molecular Phenotype
Normal Saline (Control)	Baseline vehicle	2 (++)	Moderate Brown	Normal physiological expression
Clomiphene Citrate (CC)	0.00071 mg/kg b.w.	2 (++)	Moderate Brown	Maintained baseline receptor density
CC + *Ricinus communis*	0.00071 mg/kg + 1.2 g/kg	2 (++)	Moderate Brown	Retained expression profile
Conjugated Estrogen	8.9 µg/kg b.w.	2 (++)	Moderate Brown	Sustained structural receptor pool
Ricinus communis	0.6 g/kg b.w.	2 (++)	Moderate Brown	Unaltered peripheral expression
Ricinus communis	1.2 g/kg b.w.	3 (+++)	Intense / Dark Brown	Higher staining intensity
Ricinus communis	1.8 g/kg b.w.	2 (++)	Moderate Brown	Moderate staining

DISCUSSION

This study evaluated the comparative histomorphometric dynamics and spatial estrogen receptor alterations within the uterine and ovarian compartments of adult cyclic Wistar rats under *Ricinus communis* seed extract, clomiphene citrate, and exogenous estrogen interventions. The findings demonstrate distinct pharmacological profiles for each agent, highlighting a clear contrast between central neuroendocrine regulation and peripheral tissue outcomes.

Exogenous estrogen administration (Conjugated Oestrogen) established a classic atrophic state within the uterine compartments. At the tissue level, circulating estrogens bind to local nuclear ERα receptors, activating classical genomic pathways that prompt the transcription of cell-growth genes (Farzaneh & Zarghi, 2016; Sanchez et al., 2011). However, the present histological observations showed atrophic changes, while the histomorphometric differences were not statistically significant. In the present data, conjugated oestrogen showed higher mean FSH and LH values than normal saline.

This could be the possible reasons:

The higher FSH and LH levels observed following conjugated oestrogen treatment may result from insufficient treatment duration or dose, preventing sustained negative feedback on the hypothalamic–pituitary axis. Elevated oestrogen during the late follicular phase can also induce

positive feedback, leading to increased gonadotropin secretion. Additionally, ovarian follicular dysfunction may reduce inhibin production, thereby increasing FSH release. Variations in estrous cycle stage, small sample size, and assay variability may also contribute to the observed hormonal differences.

In contrast, Clomiphene Citrate demonstrated a clear clinical paradox. As a non-steroidal SERM, CC blocks nuclear estrogen receptors in the hypothalamus, preventing the brain from sensing circulating estrogen (Mbi Feh et al., 2024; Ashrafi et al., 2005). In the present dataset, however, CC showed lower mean FSH and LH values than normal saline, although the histological observations suggested follicular development.

The lower FSH and LH concentrations observed in the clomiphene-treated group may reflect effective ovarian responsiveness, with developing follicles producing increased oestradiol and inhibin that restore negative feedback on the hypothalamic–pituitary axis. In addition, successful follicular recruitment requires only an initial rise in gonadotropins, after which dominant follicles continue to develop with lower circulating FSH and LH levels. Small sample size, estrous cycle variation, and normal biological variability may also have contributed to the observed hormonal differences.

However, clomiphene's long half-life caused a persistent direct receptor blockade in peripheral tissues (Nakamura et al., 1997). In the uterus, this counteracted the positive actions of circulating estrogens, resulting in a thin luminal epithelium and compressed endometrial stroma (Plate 2). This peripheral anti-estrogenic effect thins the uterine lining, explaining the low pregnancy rates often observed clinically despite successful ovulation induction (Nakagawa et al., 2014; Nakamura et al., 1997).

Ricinus communis seed extract presented a distinct tissue-selective profile that sets it apart from both pure exogenous estrogens and clomiphene citrate. Phytochemical analysis of the extract revealed an abundance of flavonoids and phytosterols. Plant-derived phytoestrogens interact directly with nuclear estrogen receptors (ERα and ERβ) (Kuiper et al., 1998; Joshua et al., 2020). In the uterine compartments, the extract showed ERα and ERβ staining, while most measured uterine dimensions did not differ significantly.

However, within the ovarian compartments, *Ricinus communis* extract exerted profound anti-fertility effects. Immunohistochemical analysis demonstrated ERα and ERβ immunoreactivity throughout the ovarian tissue, with staining localized within the different ovarian layers. However, because the immunohistochemical evaluation was qualitative and combined ERα and ERβ into a single scoring system, receptor-specific changes in expression or downregulation could not be determined. Follicular distribution varied among the experimental groups, with the highest number of mature follicles (45) observed in the *Ricinus communis* Linn-treated group at 1.8 g/kg. Interestingly, despite the increased number of mature follicles, the highest extract dose was associated with reduced serum FSH and LH concentrations, which may have attenuated the pre-ovulatory LH surge required for follicular rupture and ovulation. These findings suggest a dose-dependent modulation of the hypothalamic–pituitary–ovarian axis by *Ricinus communis* Linn; however, an anovulatory state could not be conclusively established based on the present data. These dual actions shielding the uterus from hyperproliferation while disrupting follicle maturation and ovulation support further

investigation of the traditional use of *Ricinus communis* seed preparations as primitive contraceptives (Brahmi et al., 2025; Raji et al., 2006).

CONCLUSION

In conclusion, this study demonstrates that the crude seed extract of *Ricinus communis* functions as a potent tissue-specific endocrine modulator in adult female Wistar rats. Histological examination revealed endometrial atrophy in the conjugated oestrogen-treated group, whereas the *Ricinus communis* Linn extract produced variable uterine histomorphological changes across the treatment groups. Clomiphene citrate also induced histological alterations in the uterine tissue; however, these changes were not accompanied by a statistically significant reduction in uterine thickness.

Within the ovarian compartments, however, *Ricinus communis* Linn extract exhibited variable ovarian ERα and ERβ immunoreactivity, accompanied by dose-dependent alterations in reproductive hormone concentrations and follicular development. These findings clarify its tissue-selective mechanisms, suggesting its potential for fertility regulation.

REFERENCES

Ashrafi, M., Ashtiani, S. K., Zafarani, F., Samani, R. O., & Eshrati, B. (2005). Evaluation of ovulation induction protocols for poor responders undergoing assisted reproduction techniques. *Saudi medical journal*, *26*(4), 593–596.

Ayodeji, A., & Roland, O. (2020). Neuroendocrine coordination of the hypothalamic-pituitary-gonadal (HPG) axis in rodent models. *Journal of Anatomical Sciences, 11*(2), 145–152.

Bancroft, J. D., & Gamble, M. (2008). *Theory and practice of histological techniques* (6th ed.). Edinburgh, Scotland: Churchill Livingstone.

Brahmi, F.; Kampemba Mujinga, F.; Guendouze, N.; Madani, K.; Boulekbache, L.; Duez, P. (2025). Benefits of Traditional Medicinal Plants to African Women's Health: An Overview of the Literature. Diseases 2025, 13, 160. https://doi.org/10.3390/diseases13050160

Farzaneh, S., & Zarghi, A. (2016). Estrogen Receptor Ligands: A Review (2013-2015). *Scientia pharmaceutica*, *84*(3), 409–427. https://doi.org/10.3390/scipharm84030409

Fedchenko, N., & Reifenrath, J. (2014). Different approaches for interpretation and quantification of immunohistochemistry images. Diagnostic Pathology, 9(1), 221–234.

Joshua, P. E., Chukwuka, R., Arazu, A. V., Godfrey, N., Ogwuegbu, M. O., & Cosmas, S. O. (2020). Phytochemical and toxicity analysis of *Ricinus communis*. *Asian Journal of Biology*, *10*(3), 34–41. https://doi.org/10.9734/AJOB/2020/v10i330109

Kuiper, G. G., Lemmen, J. G., Carlsson, B., Corton, J. C., Safe, S. H., van der Saag, P. T., van der Burg, B., & Gustafsson, J. Å. (1998). Interaction of estrogenic chemicals and phytoestrogens with estrogen receptor beta. *Endocrinology, 139*(10), 4252–4263.

Marcondes, F. K., Bianchi, F. J., & Tanno, A. P. (2002). Determination of the estrous cycle phases of rats: Some helpful considerations. *Brazilian Journal of Biology, 62*(4A), 609–614.

Matthews, J., & Gustafsson, J. Å. (2003). Estrogen receptor and receptor beta subtype-signaling mechanisms. *Molecular Interventions, 3*(5), 281–292.

Mbi Feh, M., Patterson, D., & Sterling, T. (2024). Comparative analysis of synthetic estrogens and selective estrogen receptor modulators on uterine architecture. *Toxicological Pathology, 52*(2), 189–198.

McCarty, K. S., Miller, L. S., Cox, E. B., Konrath, J., & McCarty, K. S., Jr. (1985). Estrogen receptor analyses: Correlation of biochemical and immunohistochemical methods using monoclonal antibodies. *Archives of Pathology & Laboratory Medicine, 109*(8), 716–721.

McGee, E. A., & Hsueh, A. J. (2000). Initial and cyclic recruitment of ovarian follicles. *Endocrine Reviews, 21*(2), 200–214.

Miller, L. B., Feuz, M. B., Meyer, R. G., & Meyer-Ficca, M. L. (2024). Reproductive toxicology: keeping up with our changing world. *Frontiers in toxicology*, *6*, 1456687. https://doi.org/10.3389/ftox.2024.1456687

Mitra, S., Patil, M., Patil, M., & Nayak, P. K. (2021). Pre-Ovulatory Hormones on Day of Human Chorionic Gonadotropin Trigger and Assisted Reproductive Technique Outcomes in Different Ovarian Response Groups. *Journal of human reproductive sciences*, *14*(4), 406–414. https://doi.org/10.4103/jhrs.jhrs_91_21

Nakagawa, K., Takahashi, C., & Sugiyama, R. (2014). The clomiphene citrate paradox in reproductive medicine: Central success versus peripheral failure. *Journal of Assisted Reproduction and Genetics, 31*(9), 1143–1150.

Nakamura, Y., Ono, M., Yoshida, Y., Sugino, N., Ueda, K., & Kato, H. (1997). Effects of clomiphene citrate on the endometrial thickness and echogenic pattern of the endometrium. *Fertility and sterility*, *67*(2), 256–260. https://doi.org/10.1016/S0015-0282(97)81907-3

Okwuasaba, F. K., Osunkwo, M. M., Ekwenchi, K. E., Onwukeme, K. O., Olayinka, M. O., Uguru, V. E., & Das, S. C. (1991). Anticonceptive and oestrogenic effect of a seed extract of *Ricinus communis*-Linn var. minor. Journal of Ethnopharmacology, 34(2-3), 141–145.

Patisaul, H. B., & Jefferson, W. (2010). The pros and cons of phytoestrogens. *Frontiers in Neuroendocrinology, 31*(4), 400–419.

Pelletier, G., Labrie, C., & Labrie, F. (2000). Localization of estrogen receptor alpha, estrogen receptor beta, and androgen receptors in the rat reproductive organs. *Journal of Endocrinology, 165*(2), 359–370.

Pu X, Liu L, Zhou Y and Xu Z (2024) Determination of the rat estrous cycle base on EfficientNet. Front. Vet. Sci. 11:1434991. doi: 10.3389/fvets.2024.1434991

Raji, Y., Oloyo, A. K., & Morakinyo, A. O. (2006). Effect of methanol extract of Ricinus communis seed on reproduction of male rats. *Asian journal of andrology*, *8*(1), 115–121. https://doi.org/10.1111/j.1745-7262.2006.00055.x

Sanchez, A. M., Flamini, M. I., Zullino, S., Gopal, S., Genazzani, A. R., & Simoncini, T. (2011). Estrogen receptor-{alpha} promotes endothelial cell motility through focal adhesion kinase. *Molecular human reproduction*, *17*(4), 219–226. https://doi.org/10.1093/molehr/gaq097

Taylor, C. R., & Rudbeck, L. (2013). *Immunohistochemical staining methods* (6th ed.). Carpinteria, CA: Dako.

Varghese, F., Bukhari, A. B., Malhotra, R., & De, A. (2014). IHC Profiler: An open source plugin for the quantitative evaluation and automated scoring of immunohistochemistry images of human tissue samples. *PLoS ONE*, *9*(5), e96801. https://doi.org/10.1371/journal.pone.0096801

Wolf L. J. (2000). Ovulation induction. *Clinical obstetrics and gynecology*, *43*(4), 902–915. https://doi.org/10.1097/00003081-200012000-00020

Yang, O., Kim, H. L., Weon, J. I., & Seo, Y. R. (2015). Endocrine-disrupting Chemicals: Review of Toxicological Mechanisms Using Molecular Pathway Analysis. *Journal of cancer prevention*, *20*(1), 12–24. https://doi.org/10.15430/JCP.2015.20.1.12

Yoest, K. E., Quigley, J. A., & Becker, J. B. (2019). Rapid effects of ovarian hormones on reproductive behaviors and neuroendocrine cascades. *Frontiers in Neuroendocrinology, 55*, 100–112.